

25. Sarugaser R, Lickorish D, Baksh D, Hosseini MM, Davies JE. Human umbilical cord perivascular (HUCPV) cells: a source of mesenchymal progenitors. *Stem Cells*. 2005;23:220–9.
26. Fu YS, Shih YT, Cheng YC, Min MY. Transformation of human umbilical mesenchymal cells into neurons in vitro. *J Biomed Sci*. 2004;11:652–60.
27. Fu YS, Cheng YC, Lin MY, Cheng H, Chu PM, Chou SC, et al. Conversion of human umbilical cord mesenchymal stem cells in Wharton's jelly to dopaminergic neurons in vitro: potential therapeutic application for Parkinsonism. *Stem Cells*. 2006;24:115–24.
28. Kadivar M, Khatami S, Mortazavi Y, Shokrgozar MA, Taghikhani M, Soleimani M. In vitro cardiomyogenic potential of human umbilical vein-derived mesenchymal stem cells. *Biochem Biophys Res Commun*. 2006;340:639–47.
29. Weiss ML, Medicetty S, Bledsoe AR, Rachakatla RS, Choi M, Merchav S, et al. Human umbilical cord matrix stem cells: preliminary characterization and effect of transplantation in a rodent model of Parkinson's disease. *Stem Cells*. 2006;24:781–92.
30. Chao KC, Chao KF, Fu YS, Liu SH. Islet-like clusters derived from mesenchymal stem cells in Wharton's jelly of the human umbilical cord for transplantation to control type 1 diabetes. *PLoS One*. 2008;3:1–9.
31. Carlin R, Davis D, Weiss M, Schultz B, Troyer D. Expression of early transcription factors Oct-4, Sox-2 and Nanog by porcine umbilical cord (PUC) matrix cells. *Reprod Biol Endocrinol*. 2006;4:1–13.
32. Rubinstein P, Dobrila L, Rosenfield RE, Adamson JW, Migliaccio G, Migliaccio AR, et al. Processing and cryopreservation of placental/umbilical cord blood for unrelated bone marrow reconstitution. *Proc Natl Acad Sci USA*. 1995;92:10119–22.
33. Woodbury D, Reynolds K, Black IB. Adult bone marrow stromal stem cells express germline, ectodermal, endodermal, and mesodermal genes prior to neurogenesis. *J Neurosci Res*. 2002;69:908–17.
34. Dennis JE, Merriam A, Awadallah A, Yoo JU, Johnstone B, Caplan AI. A quadripotential mesenchymal progenitor cell isolated from the marrow of an adult mouse. *J Bone Miner Res*. 1999;14:700–9.
35. Reyes M, Lund T, Lenvik T, Aguiar D, Koodie L, Verfaillie CM. Purification and ex vivo expansion of postnatal human marrow mesodermal progenitor cells. *Blood*. 2001;98:2615–25.
36. Tang DQ, Cao LZ, Burkhardt BR, Xia CQ, Litherland SA, Atkinson MA, et al. In vivo and in vitro characterization of insulin-producing cells obtained from murine bone marrow. *Diabetes*. 2004;53:1721–32.
37. Taniguchi Y, Yoshihara S, Hoshida Y, Inoue T, Fujioka T, Ikegame K, et al. Recovery from established graft-vs-host disease achieved by bone marrow transplantation from a third-party allogeneic donor. *Exp Hematol*. 2008;36:1216–25.
38. Cooke KR, Kobzik L, Martin TR, Brewer J, Delmonte J Jr, Crawford JM, et al. An experimental model of idiopathic pneumonia syndrome after bone marrow transplantation. I. The roles of minor H antigens and endotoxin. *Blood*. 1996;88:3230–9.
39. Mutin M, Dignat-George F, Sampol J. Immunologic phenotype of cultured endothelial cells: quantitative analysis of cell surface molecules. *Tissue Antigens*. 1997;50:449–58.
40. De Coppi P, Bartsch G Jr, Siddiqui MM, Xu T, Santos CC, Perin L, et al. Isolation of amniotic stem cell lines with potential for therapy. *Nat Biotechnol*. 2007;25:100–6.
41. Le Blanc K, Frassoni F, Ball L, Locatelli F, Roelofs H, Lewis I, et al. Mesenchymal stem cells for treatment of steroid-resistant, severe, acute graft-versus-host disease: a phase II study. *Lancet*. 2008;371:1579–86.
42. Spaeth EL, Dembinski JL, Sasser AK, Watson K, Klopp A, Hall B, et al. Mesenchymal stem cell transition to tumor-associated fibroblasts contributes to fibrovascular network expansion and tumor progression. *PLoS One*. 2009;4:1–11.
43. Sato K, Ozaki K, Mori M, Muroi K, Ozawa K. Mesenchymal stromal cells for graft-versus-host disease : basic aspects and clinical outcomes. *J Clin Exp Hematop*. 2010;50:79–89.

特集 知っておきたい重症産褥合併症

8. 周産期心筋症(産褥心筋症)

村林奈緒 池田智明
三重大学医学部産科婦人科学教室

要旨

周産期心筋症(産褥心筋症)は、心疾患の既往がない女性が、妊娠末期から産褥期に突然原因不明の心不全をきたし、心エコーにて拡張型心筋症様の心拡大および左室収縮能の著しい低下所見を認める疾患であり、母体死亡の原因疾患の一つである。これまで、わが国において発生状況や経過などの把握がなされていなかったため、2007年1月から2008年12月の2年間に発症した周産期心筋症についての全国調査が行われた。本稿では、この全国調査結果をもとに、周産期心筋症について解説する。

KeyWords 心筋症, 妊娠, 心不全

診断基準

周産期心筋症の診断基準はいまだ確立されていないが、下記の基準が用いられることが多い¹⁾²⁾。

- ①分娩前1カ月から分娩後5カ月に発症した心不全
- ②心不全の基礎疾患がない
- ③分娩前1カ月以前に心疾患の既往がない
- ④心エコーにて、左室機能低下所見を認める
左室駆出率(LVEF: left ventricular ejection fraction) < 45-55%
左室短縮率(%FS: percent fractioning shortening) < 30%

ただし、妊娠初期に発症した症例と末期に発症した症例の臨床所見に差がないことが報告さ

れた³⁾ため、①の発症時期については、妊娠初期から分娩後5カ月とされることもある。

原因

周産期心筋症の原因は、現在のところ明らかでないが、ウイルス感染、自己免疫機序、ホルモン異常、遺伝子異常、中毒などが原因である可能性が指摘されている⁴⁾。最近、酸化ストレスによって生じる異型プロラクチンが、心筋を障害し、心筋症を発生させると報告され⁵⁾周産期心筋症の原因として注目されている。

治療

一般的な急性心不全に準じて行う。重症例では大動脈バルーンポンピングや経皮的心肺補助

法が必要となることもある。治療抵抗性の場合、心臓移植を要する症例や、死亡に至る症例もある。

また、先に述べたように、異型プロラクチンが病因であるとの報告に対し、抗プロラクチン薬であるプロモクリプチンが周産期心筋症治療薬として有効であったと報告され⁶⁾根治療法として期待されている。

全国調査結果について

これまで出産後の心不全症例は妊産婦死亡として取り扱われてこなかったため、周産期心筋症の発症頻度や経過は把握されていなかった。しかし、現実には、周産期心筋症はわが国における妊産婦死亡の重要な原因疾患である。このため、現状を把握し、早期診断や治療法の確立につなげることを目的に、平成21年度、厚生労働科学研究の一環として、国立循環器病研究センター(研究代表者:神谷千津子)により周産期心筋症についての全国調査が行われた。以下、この調査結果報告⁷⁾に基づいて述べる。

1. 調査対象

今回の全国調査の対象者は、2007年1月から2008年12月までの2年間に新規に発症した症例で、以下の診断基準をすべて満たす者とされた。

1. 妊娠中または妊娠終了後5カ月以内に新たに心不全の症状が出現、もしくは心エコー上、左室機能の低下を認めた症例
2. 左室駆出率(LVEF)が50%未満、もしくは左室短縮率(%FS)が30%未満であること
3. ほかに心不全の原因となる疾患がないこと
4. 心疾患の既往がないこと

周産期心筋症を発症した症例の既往歴

高血圧症	14%
不整脈	5%
糖尿病	3%
喘息	3%
甲状腺機能異常	3%
周産期心筋症既往	2%

2. 発症率

調査期間の2年間で報告された症例数は102症例であった。発症年齢は平均32.7歳(22-43歳)であった。発症率は全体では約20,000分娩に1人の割合であったが、発症率が多かった35-39歳では約1万分娩に1人の割合となっていた。わが国での発症率は、米国での発症率(2,289~4,000分娩に1人)⁸⁾に比べると低かった。

3. リスクファクター

既往歴として、高血圧症が14%の症例で認められた。その他表1に示す既往歴が認められた。妊娠合併症としては、多胎(15%)、子宮収縮抑制薬使用(14%)、妊娠高血圧症(38%)がリスクファクターと考えられた。

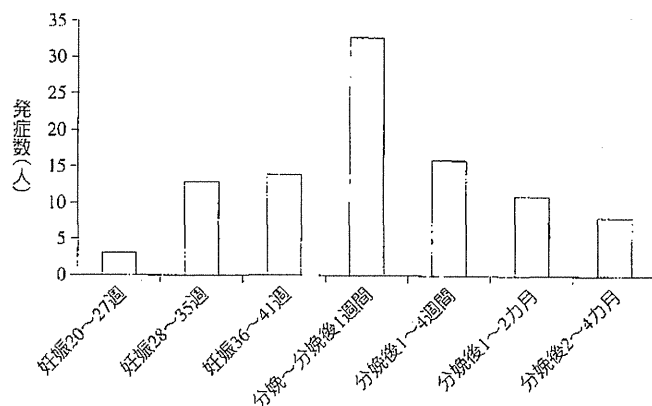
4. 発症時期

妊娠中の発症が31%、分娩後の発症が69%であった。最も多かったのは、分娩から1週間以内で33例(32.4%)であった。また、妊娠28週から分娩までに発症した症例と、分娩後1週間から2カ月までに発症した症例がそれぞれ26.5%を占めた(図1)。

5. 初発症状・所見

初発症状は呼吸困難が最も多く(80%)、咳、浮腫、倦怠感、動悸、体重増加などがこれに次いだ。しかし、息苦しさやむくみなどは、妊娠中は正常であっても聞かれる訴えであり、心不全を見逃さない姿勢が必要である。

初診時の左心機能は著明に低下しており、



〔文献8より引用・改変〕

図1 周産期心筋症を発症した時期

NYHA (New York Heart Association) class III が 24%, NYHA class IV が 54% であった。心エコー所見は、LVEF 31.6 ± 12.0 (平均値 \pm 標準偏差)%, %FS 15.8 ± 7.0 % であった。心機能低下に関連して増加が認められるホルモンである brain natriuretic peptide (BNP) の血中濃度の平均は $1,258 \pm 1,028$ pg/mL であり、BNP が 100 pg/mL 以下であったのは 4 症例のみであった。

なお、初診科は産婦人科が 63%、一般内科が 12% で、循環器科を受診したのは 9% であった。

6. 予後

102 症例のうち 4 症例 (4%) が死亡した。死亡症例の内訳は、妊娠 34 週に肺水腫をきたした症例、妊娠 37 週に分娩停止で緊急帝王切開が施行された翌日に心不全をきたした症例、経皮的心肺補助装置を使用して経膈分娩を行ったが 2 日後に心停止に至った症例、周産期心筋症と診断されたのちに徐々に状態が悪化して 6 カ月以上経過後に死亡に至った症例の 4 症例であった。

また、2% の症例で重度の左心機能の低下が認められ、左心補助装置を必要とし、心臓移植待機の状態となった。上記以外で追跡可能であった 89% の症例は、平均在院日数約 1 カ月で退院可能となった。これらの症例の退院時の心エ

コー所見は、LVEF 43.6 ± 14.1 %, %FS 22.8 ± 8.9 % であり、血中 BNP 値は 211 ± 277 pg/mL であった。

また、 9.6 ± 6.5 カ月間の経過観察後は、LVEF 54.6 ± 13.6 %, %FS 29.6 ± 8.3 % まで回復し、血中 BNP 値は 44 ± 103 pg/mL まで低下した。63% の症例で、6 カ月後には LVEF が 50% 以上に回復していた。

また、高血圧は周産期心筋症のリスクファクターと考えられてきたが、神谷らの報告⁷⁾によると、高血圧合併症例と高血圧非合併症例との比較において、発症後の平均観察期間 (高血圧合併例 7.9 カ月 vs 高血圧非合併例 10.9 カ月) における左心機能の回復は、高血圧合併例で良好であった。これは、高血圧は周産期心筋症と共存することが多いが、高血圧非合併例とは異なる病態である可能性を示唆し、高血圧合併症例を周産期心筋症に含めるべきかどうかという、診断基準に一石を投じる結果であると考えられた。

胎児の予後については、妊娠中の心不全発症例で悪化し、胎児死亡 3 例、胎児発育遅延 2 例が認められた。

次回妊娠について

周産期心筋症を発症した患者について、次回妊娠許可条件は確立されていない。

Elkayamらは、前回周産期心筋症であった44例の妊婦の調査において、今回妊娠時に心不全徴候をきたしたのは、今回妊娠前にLVEFが50%以上に回復していた症例では21%、LVEFが50%以上に回復しなかった症例では44%に認められたと報告した⁹⁾。また、Fettらは、次回妊娠許可条件はLVEFが55%以上に回復した症例とすべきと報告している¹⁰⁾。

おわりに

周産期心筋症は、今なお未解決な部分の多い疾患ではあるが、全国調査により、少しずつわが国における実態が明らかにされてきた。妊産婦死亡につながる重篤な疾患であり、産婦人科医、内科医ともに疾患の理解を深め、早期診断を行う必要がある。

また、上記の全国調査に引き続き、現在、「周産期心筋症(産褥心筋症)の発症に関する前向き研究」(研究代表者：神谷千津子)が進められている。これは、周産期心筋症についての長期予後や詳細な危険因子の解明、簡易検査(血清BNP等)およびその他の診断にかかわる検査項

目を決定し、診断時期、治療による予後の違いなどを明らかにすることを目的とする研究である。病因解明や早期発見早期治療による予後の向上につながることを期待される。

文献

- 1) Demakis JG, et al : Peripartum cardiomyopathy. *Circulation* 1971 ; 44 : 964-968.
- 2) National Heart, Lung, and Blood Institute and Office of Rare Diseases (National Institutes of Health) Workshop Recommendations and Review : Peripartum cardiomyopathy. *JAMA* 2000 ; 283 : 1183-1188.
- 3) Elkayam U, et al : Pregnancy-associated cardiomyopathy : clinical characteristics and a comparison between early and late presentation. *Circulation* 2005 ; 111 : 2050-2055.
- 4) Demakis JG, et al : Peripartum cardiomyopathy. *Circulation* 1971 ; 44 : 964-968.
- 5) Hilfiker-Kleiner D, et al : A cathepsin D-cleaved 16 kDa form of prolactin mediates postpartum cardiomyopathy. *Cell* 2007 ; 128 : 589-600.
- 6) Sliwa K, et al : Evaluation of bromocriptine in the treatment of acute severe peripartum cardiomyopathy. *Circulation* 2010 ; 121 : 1465-1473.
- 7) Kamiya CA, et al : Different characteristics of peripartum cardiomyopathy between patients complicated with and without hypertensive disorders. *Circ J* 2011 ; 75 : 1975-1981.
- 8) Sliwa K, et al : Peripartum cardiomyopathy. *Lancet* 2006 ; 368 : 687-693.
- 9) Elkayam U, et al : Maternal and fetal outcomes of subsequent pregnancies in women with peripartum cardiomyopathy. *N Engl J Med* 2001 ; 344 : 1567-1571.
- 10) Fett JD, et al : Risk of heart failure relapse in subsequent pregnancy among peripartum cardiomyopathy mothers. *Int J Gynecol Obstet* 2010 ; 109 : 34-36.

著者連絡先

〒514-8507
三重県津市江戸橋2丁目174番地
三重大学医学部産科婦人科学教室
村林奈緒



Febuxostat suppressed renal ischemia–reperfusion injury via reduced oxidative stress

Hidetoshi Tsuda^a, Noritaka Kawada^b, Jun-ya Kaimori^{a,b}, Harumi Kitamura^b, Toshiki Moriyama^b, Hiromi Rakugi^b, Shiro Takahara^a, Yoshitaka Isaka^{b,*}

^a Department of Advanced Technology for Transplantation, Osaka University Graduate School of Medicine, Suita, Japan

^b Department of Geriatric Medicine and Nephrology, Osaka University Graduate School of Medicine, Suita, Japan

ARTICLE INFO

Article history:

Received 30 August 2012

Available online 17 September 2012

Keywords:

Apoptosis

Febuxostat

Ischemia–reperfusion injury

Kidney

ABSTRACT

Febuxostat is a novel selective inhibitor of xanthine oxidase (XO), approved for treating hyperuricemia. XO inhibits the generation of uric acid (UA) as well as the resulting generation of superoxide. During renal ischemia–reperfusion (I/R) injury, the burst of reactive oxygen species (ROS) can trigger the inflammation and the tubular cell injury. As XO is a critical source of ROS, inhibition of XO could be a therapeutic target for I/R injury. Therefore, we performed this study to test the therapeutic effect of febuxostat on renal I/R injury.

Sprague–Dawley rats, received vehicle or febuxostat, were subjected to right nephrectomy and left renal I/R injury. Febuxostat significantly suppressed XO activity, and thereby reduced oxidative stress, assessed by nitrotyrosine, thiobarbituric acid-reactive substances (TBARS) and urine 8-isoprostane. Furthermore, febuxostat reduced the induction of endoplasmic reticulum (ER) stress, assessed by GRP-78, ATF4, and CHOP. Vehicle-treated I/R injured rats exhibited elevated serum creatinine and UN, which were significantly suppressed in febuxostat-treated I/R-injured rats. Histological analysis revealed that febuxostat-treated rats showed less tubular injury and interstitial fibrosis with reduction in ED1-positive macrophage infiltration, TUNEL positive apoptotic tubular cells, and interstitial smooth muscle α actin (SM α A) expression, compared to vehicle-treated rats. In conclusion; novel XO inhibitor, febuxostat, can protect kidney from renal I/R injury, and may contribute to preserve kidney function.

© 2012 Elsevier Inc. All rights reserved.

1. Introduction

Renal ischemia–reperfusion (I/R) injury, frequently associated with shock or surgery, is a major cause of acute renal failure [1]. Reactive oxygen species (ROS) have been implicated as a major pathophysiological component in I/R injury in several tissues including kidney [2]. Several lines of insights have focused on xanthine oxidoreductase (XOR) inhibitor as a therapeutic tool for I/R injury. XOR inhibits the generation of uric acid (UA) as the final product of purine catabolism, as well as the resulting generation of superoxide. Under ischemic condition, adenosine triphosphate (ATP) is degraded to xanthine, and hypoxanthine, which are substrates for XOR. XOR functions as either xanthine dehydrogenase (XDH) form, which transfers electron to NAD⁺, and generates NADH or xanthine oxidase (XO) form, which transfers electron to O₂ and generates oxidative stress. Because ischemia-induced cellu-

lar calcium overload convert XDH to XO [3], under reperfusion phase, enhanced XO can produce more ROS, such as superoxide, hydrogen peroxide, and hydroxyl radicals. These ROS can exaggerate cellular damages.

Recently, apoptosis is triggered by ROS-mediated activation of endoplasmic reticulum (ER) stress requiring involvement of CHOP pathway [4]. Disturbances such as hypoxia and oxidative stress may lead to ER dysfunction, which can induce ER stress in kidney [5]. Oxidative stress can cause aberrant unfolded and misfolded proteins, which in turn induces ER stress. Some unfolded protein responses enhance the protein-folding capacity by activating the transcription of target genes, such as glucose-regulated protein-78 (GRP-78) [6]. ER stress-induced apoptosis is mainly mediated C/EBP homologous protein-10 (CHOP). CHOP is a transcription factor, which induces several proapoptotic factors, and is downstream of activating transcription factor-4 (ATF4). Severe ER stress preferentially induces proapoptotic CHOP expression as compared to mild ER stress [5].

On the basis that XO produces ROS, XOR inhibitor might have a protective effect under renal I/R injury. Allopurinol, one of XOR inhibitor, is a classic “suicide inhibitor,” as its binding to and

* Corresponding author. Address: Department of Geriatric Medicine and Nephrology, Osaka University Graduate School of Medicine, Suita, Osaka 565-0871, Japan. Fax: +81 6 6879 3857.

E-mail address: isaka@kid.med.osaka-u.ac.jp (Y. Isaka).

reduction of the molybdenum (Mo) cofactor induces self-oxidation to form oxypurinol, an active inhibitory metabolite. Reduction of the Mo cofactor by allopurinol ultimately leads to electron transfer to the FAD, resulting in the ROS production [7]. In addition, oxypurinol binding and resultant inhibition also requires the Mo cofactor to be reduced [8]. In this point of view, both allopurinol and oxypurinol require enzyme turnover resulting in ROS formation before inhibition is attained. On the contrary, a new XOR inhibitor, febuxostat, is not affected by the above enzyme redox state and interaction with XO, and thereby produces less ROS. In this study, we examined whether treatment with febuxostat could protect the kidney from tubular ROS production under renal ischemia–reperfusion injury and, thereby, inhibit subsequent tubulointerstitial injury.

2. Materials and methods

2.1. Experimental design

Male Sprague–Dawley rats weighing 200 g were purchased from Japan SLC Inc. (Shizuoka, Japan) and were maintained under standard conditions until the experiments were done. All studies were performed in accordance with the principles of the Guideline on Animal Experimentation of Osaka University. The rats were randomly allocated into three groups: (1) vehicle-treatment group (Veh group); (2) febuxostat-treatment group (Feb group) and (3) sham-operated group (sham group). Vehicle and febuxostat group rats received orally 0.5 ml of 0.5% methylcellulose as a vehicle and 10 mg/kg/day of febuxostat in 0.5% methylcellulose 1 day and 60 min before I/R injury, respectively. On day 0, the rats were subjected to right renal nephrectomy and left renal I/R injury. Sham-operated rats were used as normal control. All rats were anesthetized with an intraperitoneal injection of sodium thiopentone (30 mg/kg). The animals were allowed to stabilize for 30 min before they were subjected to right nephrectomy and 45 min of left renal occlusion using artery clips to clamp the renal pedicles. Occlusion was confirmed visually by a change in the color of the kidneys to a paler shade. Reperfusion was initiated with the removal of the artery clips and was confirmed visually by noting a blush. The rats were sacrificed 4 h ($n = 5$ in each group), 24 h ($n = 8$ in each group), and 72 h ($n = 8$ in each group) after reperfusion.

2.2. Xanthine oxidoreductase/xanthine oxidase activity

XOR activity was determined with a fluorometric assay described by Beckman et al. Briefly, kidney tissue was homogenized and centrifuged at 12,000g for 15 min. The supernatant was used to the assay based on the conversion of pterin to a fluorescent product, isoxanthopterin (Excitation wave length: 355 nm, Emission wave length: 405 nm), and was performed with or without methylene blue to determine XOR (XO + XDH) activity and XO activity, respectively.

2.3. Antibodies

Specific polyclonal antibodies for anti-smooth muscle α actin (SM α A) antibody (EPOS System: clone 1A4; Dako, Glostrup, Denmark), and anti-rat ED1 antibody (1:100, clone ED1; MCA341R, AbD Serotec, Kidlington, Oxford, UK) for macrophage staining were used in this study.

2.4. Morphology and Immunohistochemical staining

Following fixation with 4% paraformaldehyde, the kidneys were processed to paraffin and histological sections (2 μ m) of the kid-

neys were used for Periodic acid–Schiff (PAS), or for Immunohistochemical staining. Immunohistochemical staining was carried out by standard avidin–biotinylated peroxidase complex method (DakoCytomation LSAB2 System-HRP, Dako) with diaminobenzidine as the chromogen.

We have scored and calculated the number of infiltrated macrophages, and the percentage of SM α A staining positive areas by using a computer-aided manipulator (Win Roof; Mitani, Fukui, Japan). All of the slides were highlighted on digitized images using a computer-aided manipulator (Light microscopy; Nikon Eclipse 80i (Nikon, Tokyo, Japan), and pictures were taken with Nikon ACT-1 ver.2.63) Glomeruli and large vessels were excluded in the microscopic fields for image analysis. PAS-stained sections were scored by calculation of percentage of tubules in corticomedullary junction that displayed cell necrosis, loss of brush border, cast formation, and tubular dilation as follows: 0, none; 1, <10%; 2, 11–25%; 3, 26–45%; 4, 46–75%; and 5, >76%. At least 20 randomly selected areas per rat were assessed. The scores of ten fields per each kidney sections were averaged and used as the score of individual rat.

2.5. Terminal deoxynucleotidyltransferase-mediated dUTP nick end-labeling (TUNEL) staining

TUNEL staining was performed using the *in situ* Apoptosis Detection Kit (Takara Bio, Otsu, Japan), according to the manufacturer's instructions. Briefly, the sections were deparaffinized and treated with antigen retrieval in preheated 10 mmol/L sodium citrate (pH 7), using a steamer for 40 min. They were then incubated with 3% H₂O₂ for 10 min, which was followed by incubation with TdT enzyme solution for 90 min at 37 °C. The reaction was terminated by incubation in a stop/wash buffer for 30 min at 37 °C. The number of TUNEL-positive cell nuclei and the total numbers of cell nuclei stained with hematoxylin were counted in 10 random areas, and the percentages of the numbers of TUNEL-positive nuclei to the numbers of total cell nuclei were then calculated.

2.6. Real-time quantitative polymerase chain reaction (PCR)

Total RNA was extracted from the kidney cortex using an RNeasy mini kit (Qiagen, Hilden, Germany), and was reverse transcribed to cDNA. Gene expression was measured by real-time quantitative PCR using an Applied Biosystems Prism 7500 (Applied Biosystems, Foster City, CA, USA) with cDNA, SYBR Green PCR Core Reagents (Invitrogen) and a set of primers. Primers were as follows: Monocyte Chemoattractant Protein-1 (MCP-1); 5'-atgcagtaatgcccactc-3' (forward), 5'-ttccttattggggtcagcac-3' (back), IL-1 β ; 5'-caggaaggcagtgctactca-3' (forward), 5'-aaagaagggtcctggctcct-3' (back), Transforming Growth Factor- β (TGF- β); 5'-ctactgctcagctccacagaga-3' (forward), 5'-acctggggtgacgacc-3' (back), Type I collagen; 5'-aatggtgctcctgattgc-3' (forward), 5'-aatggtgctcctgattgc-3' (back), ATF4; 5'-gctatggatgggttggtcag-3' (forward), 5'-agctcatctggcatggttcc-3' (back), CHOP; 5'-ttacagtcagtcagctgagtc-3' (forward), 5'-gacctcctgcagatcctcatac-3' (back), GRP-78; 5'-tgttccgctctaccatgaac-3' (forward), 5'-aattcgagtagatccgcaac-3' (back), 18s rRNA; 5'-gcaattatccccatgaacg-3' (forward), 5'-ggcctcactaaaccatcaac-3' (back). 18s rRNA transcript was used as an internal control.

2.7. Oxidative stress

Kidney cortex tissue was weighted and homogenized with 0.05 M potassium phosphate buffer containing 1 mM ethylenediaminetetraacetic acid (EDTA) and protease inhibitor cocktail (Roche Applied Science, Indianapolis, USA). Tissue suspension was centrifuged at 12,000 \times g for 15 min at 4 °C, and the supernatants were collected and used for assay. Nitrotyrosine levels were quantified by enzyme immunoassay using the NWLSS nitrotyro-

sine ELISA kit (Northwest Life Science Specialties, LLC) according to the manufacturer's instructions. The measurement of thiobarbituric acid-reactive substances (TBARS) in the rat kidney was based on the formation of malondialdehyde by using a commercially available TBARS Assay kit (Cayman Chemical) according to the manufacturer's instructions.

Urinary concentrations of 8-isoprostane was determined using enzyme immunoassay kits from Japan institute for the control of aging (Shizuoka, Japan.). Results were adjusted by urine creatinine concentration, and averaged.

2.8. Statistical analysis

All values are expressed as mean \pm SE. Comparisons between two parameters were analyzed by using the unpaired Student's *t*-test. Comparisons among the three groups were evaluated using the Tukey method by GraphPad Prism version 4.0 for Windows (GraphPad Software, San Diego, CA, USA), and *P* < 0.05 was considered to be statistically significant.

3. Results

3.1. Febuxostat suppressed renal XO and XDH activity

Renal tissue XO activity was not changed in vehicle-treated ischemia–reperfusion (I/R)-injured kidneys ($1124 \pm 187 \mu\text{U}/\text{mg}$ protein) compared with sham-operated kidney ($1390 \pm 397 \mu\text{U}/\text{mg}$ protein) 4 h after I/R injury. In contrast, XO activity was not detected in febuxostat-treated kidneys. Concomitant with the reduction of XO activity, febuxostat significantly reduced UA levels ($0.3 \pm 0.0 \text{ mg/dL}$) compared with vehicle treatment ($1.4 \pm 0.1 \text{ mg/}$

dL) 4 h after I/R injury, but no difference was observed at 24 h between vehicle-treated and febuxostat-treated group (0.50 ± 0.14 and $0.58 \pm 0.07 \text{ mg/dL}$, respectively).

3.2. Febuxostat inhibits oxidative stress and ER stress

As we observed the sufficient XO inhibition of febuxostat in I/R injured kidneys, we examined the resultant effect on oxidative stress. Nitrotyrosine concentration, a marker of nitro-oxidative stress, extracted from febuxostat-treated I/R-injured kidneys was lower ($11.9 \pm 2.6 \text{ pmol/g}$ tissue) than that from vehicle-treated kidney ($30.7 \pm 5.4 \text{ pmol/g}$ tissue) 4 h after disease induction (*P* < 0.05 vs. Veh group; Fig. 1A). Febuxostat treatment also significantly suppressed TBARS concentration, a marker of lipid peroxidation, ($28.5 \pm 3.7 \text{ nmol/g}$ tissue) compared with vehicle treatment ($37.6 \pm 3.0 \text{ nmol/g}$ tissue) 4 h after disease induction (*P* < 0.05 vs. Veh group; Fig. 1B). In addition, urinary excretion of 8-isoprostane was also significantly suppressed febuxostat-treated rats compared with vehicle-treated rats (1.83 ± 0.09 and $2.98 \pm 0.44 \text{ ng/mg Cr}$, respectively, *P* < 0.05; Fig. 1C).

Several studies have indicated that oxidative stress induces ER stress [5]. Therefore, the expression of ER stress-related genes in kidney tissues was measured 4 h after I/R. RT-PCR demonstrated that marked elevation in GRP-78 (Fig. 1D), ATF4 (Fig. 1E), and CHOP (Fig. 1F) levels were observed in the vehicle-treated I/R injury model rats (3.43 ± 0.60 -, 2.88 ± 0.77 -, and 4.07 ± 0.55 -fold, respectively, *P* < 0.05) compared with the sham group (1.19 ± 0.37 -, 1.00 ± 0.05 -, and 1.06 ± 0.09 -fold, respectively). In contrast, I/R injury-induced ER stress was suppressed in the Feb treated group (1.29 ± 0.30 -, 0.70 ± 0.33 -, and 1.95 ± 0.34 -fold, respectively, *P* < 0.05 vs. Veh group).

3.3. Effects on tubular damage and apoptosis in the I/R injury kidney

I/R-injured rats exhibited impaired renal function, assessed by serum UN and creatinine ($95.9 \pm 8.9 \text{ mg/dL}$ and $1.59 \pm 0.19 \text{ mg/dL}$, respectively, *P* < 0.01 vs. sham group), compared with sham-operated rats ($17.2 \pm 0.8 \text{ mg/dL}$ and $0.36 \pm 0.04 \text{ mg/dL}$, respectively). Febuxostat ameliorated the elevated serum UN and creatinine levels (38.2 ± 4.3 and $0.62 \pm 0.06 \text{ mg/dL}$, respectively, *P* < 0.01 vs. Veh group) (Fig. 2A).

PAS staining of kidney sections from vehicle-treated rats 24 h after I/R injury showed marked disruption, including widespread degeneration of tubular architecture, tubular swelling, luminal congestion, loss of brush border, and increased interstitial infiltration (PAS score; 3.4 ± 0.1 , Fig. 2B). Treatment with febuxostat ameliorated characteristic histological changes of I/R injury, including tubular damage and increased interstitial cells (PAS score; 1.8 ± 0.1 , *P* < 0.001 vs. Veh group, Fig. 2C). To elucidate the protective mechanisms by which febuxostat administration ameliorated tubular injury, we did TUNEL staining to quantify the number of apoptotic cells. In the vehicle-treated I/R injury model rats, TUNEL-positive, apoptotic cells increased among the tubular epithelial cells at 24 h (TUNEL-positive cells per all nuclei, $9.02 \pm 0.27\%$, Fig. 2D), while TUNEL-positive, apoptotic cells were significantly decreased by febuxostat treatment ($1.23 \pm 0.06\%$, *P* < 0.001 vs. Veh group, Fig. 2E).

3.4. Febuxostat ameliorates interstitial infiltration

As we observed the reduced interstitial infiltrated cells in febuxostat-treated kidney, we then examined the macrophage infiltration in the interstitium. The number of ED-1 positive macrophages was significantly increased in interstitial area of vehicle-treated I/R-injured kidneys at 24 h and 72 h (266.3 ± 17.1 and 503.6 ± 19.0 per low power field (LPF), respectively, *P* < 0.001

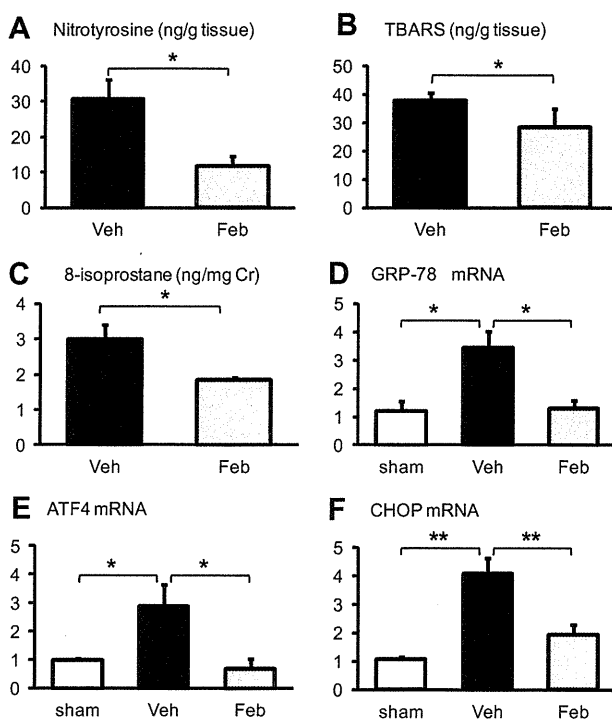


Fig. 1. Effect febuxostat on oxidative stress. ELISA demonstrated the renal concentration of nitro-tyrosine (A) and TBARS (B), and urinary excretion of 8-isoprostane (C) 4 h after I/R injury (*P* < 0.05). Real-time PCR showed GRP-78 (D), ATF4 (E), and CHOP (F) mRNA expression 4 h after I/R injury. Result was expressed as relative expression against the expression in sham-operated rats (**P* < 0.05, ***P* < 0.01).

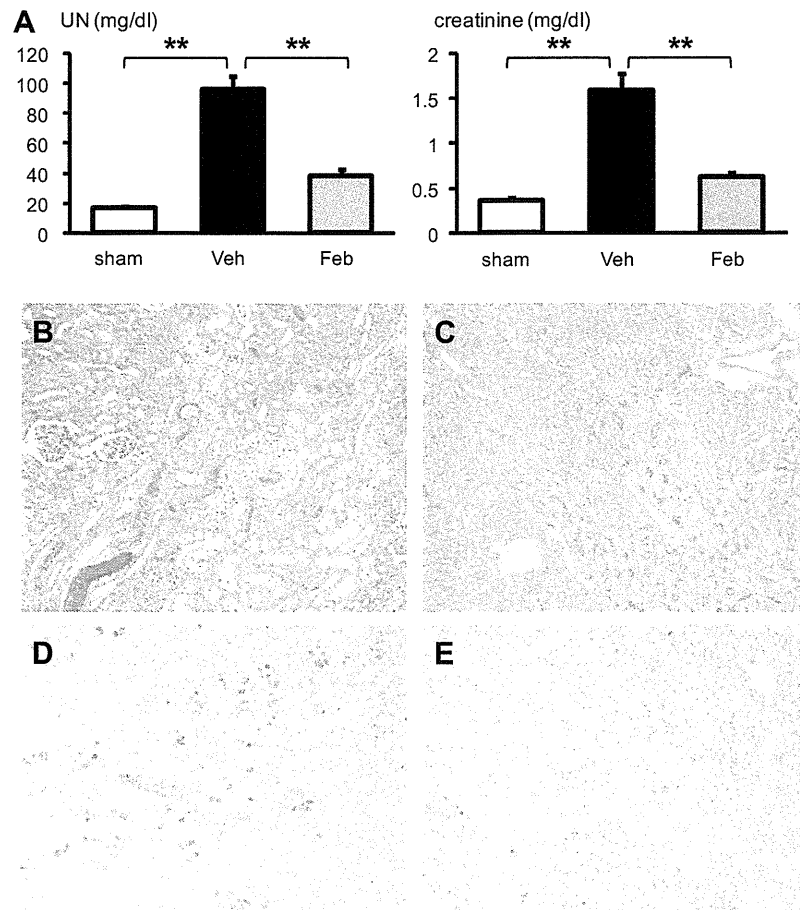


Fig. 2. Effects of febuxostat on renal injury. Effect of febuxostat on renal function was summarized. Serum UN and creatinine were examined 24 h after sham-operation (sham) or ischemia–reperfusion injury with heminephrectomy treated with vehicle (Veh) or febuxostat (Feb) (A) (** $P < 0.01$). Effect of febuxostat on tubular injury was assessed by staining with PAS (B, C) or TUNEL (D, E) from vehicle-treated (B, D) or febuxostat-treated (C, E) I/R injured rats. (magnification, 200 \times).

vs. sham group) compared with sham-operated kidneys (8.6 ± 0.6 field and 25.8 ± 2.9 per LPF, respectively), while febuxostat suppressed the infiltration of ED-1-positive macrophages (81.1 ± 7.6 and 228.9 ± 11.8 per LPF, respectively, $P < 0.001$ vs. Veh group) (Fig. 3A–C), which was consistent with the observation from PAS staining. As we observed the protective effect of febuxostat on macrophage infiltration, we examined the effect of febuxostat on MCP-1 expression in I/R-injured kidneys. Real-time RT-PCR revealed that MCP-1 mRNA expression was increased at 4 h and 24 h in I/R-injured kidney (8.85 ± 1.82 -fold and 5.60 ± 1.42 -fold, respectively, $P < 0.01$ vs. Sham group). Parallel with the significant reduction of macrophage infiltration, febuxostat suppressed the increment of MCP-1 expression (3.47 ± 0.74 -fold and 3.24 ± 0.78 -fold, respectively, $P < 0.05$ vs. Veh group) (Fig. 3D). Moreover, the IL-1 β mRNA expression, a proinflammatory cytokine that related to macrophage infiltration, was also decreased in febuxostat treated rats (1.42 ± 0.40 -fold, vs. Veh group 3.60 ± 0.65 -fold, $P < 0.05$, Fig. 3E).

3.5. Effects on interstitial phenotypic changes in the I/R injury kidney

To detect interstitial myofibroblasts, which are associated with interstitial damage and fibrosis, the expression of SM α A was examined immunohistochemically. The interstitial expression of SM α A increased 72 h after I/R injury in the vehicle-treated rats ($7.08 \pm 0.15\%$, $P < 0.001$ vs. sham group), while febuxostat treat-

ment significantly suppressed interstitial expression of SM α A ($3.63 \pm 0.12\%$, $P < 0.001$ vs. Veh group) (Fig. 4A–C). Similarly, real-time RT-PCR analysis showed that febuxostat significantly decreased TGF- β mRNA expression at 24 h after reperfusion (0.91 ± 0.14 -fold, vs. Veh group 1.35 ± 0.12 -fold, $P < 0.05$ vs. Veh group, Fig. 4D), and decreased type I collagen mRNA expression at 72 h after reperfusion (1.56 ± 0.45 -fold, vs. Veh group 4.12 ± 0.45 -fold, $P < 0.05$ vs. Veh group, Fig. 4E).

4. Discussion

We demonstrated that febuxostat suppressed XO activity, reduced oxidative stress, and thereby ameliorated tubulointerstitial injury in a rat model of I/R injury. Untreated I/R-injured kidneys exhibited increased plasma creatinine, tubular apoptosis, interstitial macrophage infiltration and interstitial SM α A expression, while administration of febuxostat ameliorated these manifestations. Importantly, febuxostat reduced oxidative stress, assessed by nitrotyrosine, TBARS and urine 8-isoprostane, together with the reduction of XO activity. Nitrotyrosine is a tyrosine nitration product mediated especially under proinflammatory conditions by reactive nitrogen species. Peroxynitrite anion: ONOO $^-$ is one of the most powerful reactive oxygen species that is produced by the reaction of nitric oxide and superoxide radicals, and considered as a marker of reactive nitrogen species induced by iNOS accompanied with oxidative stress [9]. TBARS, a measure of lipid

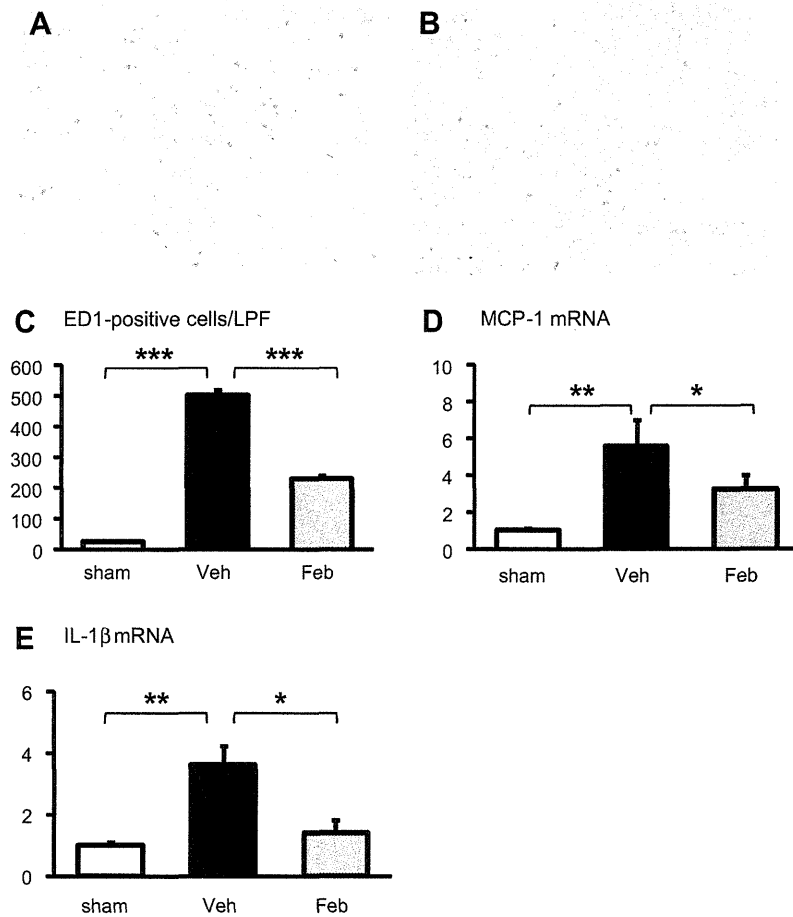


Fig. 3. Effects of febuxostat on macrophage infiltration. Representative immunohistochemical staining for ED-1-positive macrophages from vehicle-treated (A) or febuxostat-treated (B) I/R injured rats, and the number of ED-1 positive cells in interstitial space per 200 \times magnifier fields (C) 72 h after I/R injury. Real-time PCR showed the MCP-1 mRNA level at 24 h (D) and IL-1 β level at 4 h (E) after I/R injury. Result was expressed as relative expression against the expression in sham-operated rats (* $P < 0.05$, ** $P < 0.01$, *** $P < 0.001$).

peroxidation, was increased after I/R injury, but ameliorated in febuxostat-treated kidney. Racasan reported that infusion of XO increased urinary excretion of TBARS, which was completely normalized in the recovery period [10]. This observation was consistent with our results that inhibition of XO by febuxostat reduced renal TBARS. In addition, reduced 8-isoprostane revealed that febuxostat inhibited the production of the oxidative stress-mediated peroxidation of arachidonic acid. We identified less production of ROS in febuxostat-treated I/R kidneys which may originate from complete blockade of XO activity. Several lines of insights have focused on XO as a source for ROS production. XDH, which is unable to generate ROS, is converted to XO by cellular calcium overload [3]. XO can produce ROS, such as superoxide, hydrogen peroxide, and hydroxyl radicals. As we showed that febuxostat diminished the XO activity compared with the vehicle-treated I/R kidney, the reduction of XO activity might suppress renal content of nitrotyrosine and TBARS, and urinary excretion of 8-isoprostane in febuxostat-treated I/R kidneys.

We also showed that the macrophage infiltration on day 1 after increasing oxidative stress 4 h after disease induction. Previous report showed a positive interaction between ROS and macrophage infiltration. Oxidative stress promotes the expression of various inflammation-related molecules, including MCP-1 and IL-1 β , which, in turn, promotes the inflammatory cell infiltration [11]. It has been reported that XO-induced oxidative stress stimulates

MCP-1 and IL-1 β expression [12,13]. It was also reported that hyperlipidemia caused XO activity in relation to MCP-1 expression in kidney, followed by macrophage infiltration and tubulointerstitial injury, but that inhibition of XO prevented interstitial macrophage infiltration, together with decreased MCP-1 expression [12]. These results points to an important role of XO in the early stage of I/R injury, mediating macrophage infiltration by a putative oxidative stress-dependent up-regulation of MCP-1 and IL-1 β .

Together with the reduction of macrophage infiltration, TUNEL-positive apoptotic tubular cells were also suppressed in febuxostat-treated I/R kidneys on day 1, which was also consistent with the reduction of XO activity. XO-derived ROS generation was reported to induce apoptosis in cultured hepatocytes [14]. One possible mechanism of XO inhibitor-induced beneficial effect is the preservation of mitochondrial function by protecting mitochondrial membrane integrity [15]. This is supported by our observation that febuxostat-treatment decreased lipid peroxidation, assessed by TBARS concentration. In addition, febuxostat may provide beneficial effect by reducing intracellular uric acid production. In contrast to the role of plasma uric acid as a strong anti-oxidant [16], intracellular uric acid induces oxidative stress by the activation of NADPH oxidase [17], and promotes inflammation. Another possibility of suppressed apoptotic cells by febuxostat is mediated by the suppression of CHOP expression. CHOP has been identified

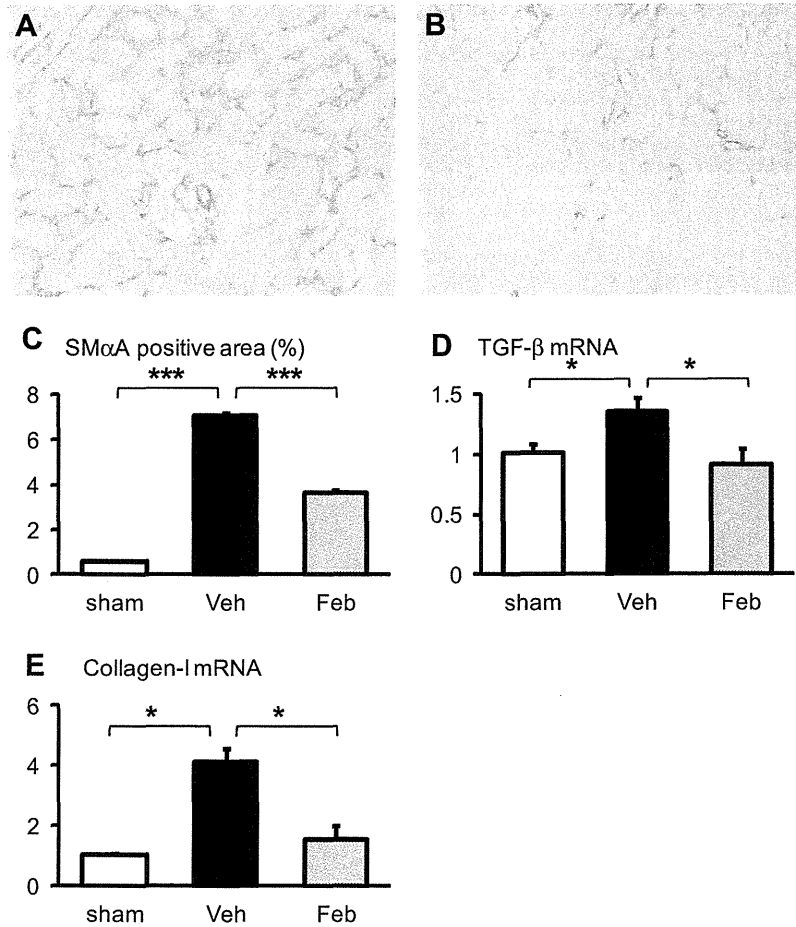


Fig. 4. Effects of febuxostat on phenotypic alteration. Representative immunohistochemical staining for SM α A from vehicle-treated (A) or febuxostat-treated (B) I/R injured rats, and the percentage of SM α A positive staining areas in interstitial space (C) 72 h after I/R injury. (magnification, 200 \times) Real-time PCR showed the TGF- β mRNA expression at 24 h (D) and type I collagen mRNA expression at 72 h (E) after I/R injury. Result was expressed as relative expression against the expression in sham-operated rats (* $P < 0.05$, *** $P < 0.001$).

as an ER-initiated proapoptotic signal that plays an important role in the pathogenesis of diabetes mellitus and neurodegenerative diseases [18]. In kidney, apoptosis is triggered by ROS-mediated activation of CHOP pathway [4]. We previously demonstrated that unfolded protein accumulation was observed in I/R-injured kidney tubules [19], and here showed that GRP-78, target gene of unfolded protein response, was upregulated in I/R kidney, but febuxostat reversed this induction. In addition, ATF4, and its downstream CHOP were increased in I/R kidney, while treatment of febuxostat ameliorated their increase. Thus, febuxostat suppressed apoptosis by inhibiting oxidative stress and ER stress.

The present study supports the current pathological concept that XO activity itself rather than hyperuricemia may play important roles in I/R injury. Several reports suggest the UA-independent therapeutic effect of XO inhibitor. Clinical study showed that benzbromaron lowered UA level, but had no effects on hemodynamic impairment in chronic heart failure patients [20]. XO inhibitor showed renoprotective effects in 5/6 nephrectomy rats without hyperuricemia [21]. Since XO are expressed ubiquitously, targeting XO activity can be applied to a variety of tissue and disease conditions. CKD patients are shown to have high oxidative stress [22], and those patients are expected to have high protein conversion rate from XDH to XO. The use of XO inhibitor in CKD patients has been restricted due to the lack of appropriate agents, but we now have novel agent; febuxostat, which can be used effectively

even in CKD patients. Thus, we need further investigations about the role of febuxostat in the progression of CKD. Although the reduction of uric acid itself may be protective for CKD patients, uric acid-independent actions of XO inhibitor may play significant roles on the progression of CKD or CVD. It may eventually support the idea to apply XO inhibitors not only to hyperuricemic, but also to non-hyperuricemic subjects to modulate these UA-independent actions of XO.

In conclusion, our results show that XO activity contributes to the progression of renal interstitial injury by modulating oxidative stress and ER stress. Our observations support the current pathological concept that, in addition to hyperuricemia, increased XO activity itself may play important roles in the progressive renal injury, and a novel XO inhibitor, febuxostat, may be a therapeutic tool for progressive renal injury.

References

- [1] F. Gueler, W. Gwinner, A. Schwarz, H. Haller, Long-term effects of acute ischemia and reperfusion injury, *Kidney Int.* 66 (2004) 523–527.
- [2] M.S. Paller, J.R. Hoidal, T.F. Ferris, Oxygen free radicals in ischemic acute renal failure in the rat, *J. Clin. Invest.* 74 (1984) 1156–1164.
- [3] J.M. McCord, Oxygen-derived free radicals in postischemic tissue injury, *N. Engl. J. Med.* 312 (1985) 159–163.
- [4] W. Ding, L. Yang, M. Zhang, Y. Gu, Reactive oxygen species-mediated endoplasmic reticulum stress contributes to aldosterone-induced apoptosis

- in tubular epithelial cells, *Biochem. Biophys. Res. Commun.* 418 (2012) 451–456.
- [5] R. Inagi, Endoplasmic reticulum stress in the kidney as a novel mediator of kidney injury, *Nephron Exp. Nephrol.* 112 (2009) e1–e9.
- [6] M. Ni, A.S. Lee, ER chaperones in mammalian development and human diseases, *FEBS Lett.* 581 (2007) 3641–3651.
- [7] C. Galbusera, P. Orth, D. Fedida, T. Spector, Superoxide radical production by allopurinol and xanthine oxidase, *Biochem. Pharmacol.* 71 (2006) 1747–1752.
- [8] V. Massey, H. Komai, G. Palmer, G.B. Elion, On the mechanism of inactivation of xanthine oxidase by allopurinol and other pyrazolo[3,4-d]pyrimidines, *J. Biol. Chem.* 245 (1970) 2837–2844.
- [9] I. Mohiuddin, H. Chai, P.H. Lin, A.B. Lumsden, Q. Yao, C. Chen, Nitrotyrosine and chlorotyrosine: clinical significance and biological functions in the vascular system, *J. Surg. Res.* 133 (2006) 143–149.
- [10] S. Racasan, E. Turkstra, J.A. Joles, H.A. Koomans, B. Braam, Hypoxanthine plus xanthine oxidase causes profound natriuresis without affecting renal blood flow autoregulation, *Kidney Int.* 64 (2003) 226–231.
- [11] M.J. Paul-Clark, S.K. McMaster, R. Sorrentino, S. Srisikandan, L.K. Bailey, L. Moreno, B. Ryffel, V.F. Quesniaux, J.A. Mitchell, Toll-like receptor 2 is essential for the sensing of oxidants during inflammation, *Am. J. Respir. Crit. Care Med.* 179 (2009) 299–306.
- [12] W. Gwinner, H. Scheuer, H. Haller, R.P. Brandes, H.J. Groene, Pivotal role of xanthine oxidase in the initiation of tubulointerstitial renal injury in rats with hyperlipidemia, *Kidney Int.* 69 (2006) 481–487.
- [13] M. Romagnoli, M.C. Gomez-Cabrera, M.G. Perrelli, F. Biasi, F.V. Pallardo, J. Sastre, G. Poli, J. Vina, Xanthine oxidase-induced oxidative stress causes activation of NF-kappaB and inflammation in the liver of type I diabetic rats, *Free Radical Biol. Med.* 49 (2010) 171–177.
- [14] S. Sakuma, M. Negoro, T. Kitamura, Y. Fujimoto, Xanthine oxidase-derived reactive oxygen species mediate 4-oxo-2-nonenal-induced hepatocyte cell death, *Toxicol. Appl. Pharmacol.* 249 (2010) 127–131.
- [15] W.Y. Lee, S.M. Lee, Synergistic protective effect of ischemic preconditioning and allopurinol on ischemia/reperfusion injury in rat liver, *Biochem. Biophys. Res. Commun.* 349 (2006) 1087–1093.
- [16] G.K. Glantzounis, E.C. Tsimoyiannis, A.M. Kappas, D.A. Galaris, Uric acid and oxidative stress, *Curr. Pharm. Des.* 11 (2005) 4145–4151.
- [17] Y.Y. Sautin, T. Nakagawa, S. Zharikov, R.J. Johnson, Adverse effects of the classic antioxidant uric acid in adipocytes: NADPH oxidase-mediated oxidative/nitrosative stress, *Am. J. Physiol. Cell Physiol.* 293 (2007) C584–C596.
- [18] S.J. Marciniak, C.Y. Yun, S. Oyadomari, I. Novoa, Y. Zhang, R. Jungreis, K. Nagata, H.P. Harding, D. Ron, CHOP induces death by promoting protein synthesis and oxidation in the stressed endoplasmic reticulum, *Genes Dev.* 18 (2004) 3066–3077.
- [19] T. Kimura, Y. Takabatake, A. Takahashi, J.Y. Kaimori, I. Matsui, T. Namba, H. Kitamura, F. Niimura, T. Matsusaka, T. Soga, H. Rakugi, Y. Isaka, Autophagy protects the proximal tubule from degeneration and acute ischemic injury, *J. Am. Soc. Nephrol.* 22 (2011) 902–913.
- [20] K. Ogino, M. Kato, Y. Furuse, Y. Kinugasa, K. Ishida, S. Osaki, T. Kinugawa, O. Igawa, I. Hisatome, C. Shigemasa, S.D. Anker, W. Doehner, Uric acid-lowering treatment with benzbromarone in patients with heart failure: a double-blind placebo-controlled crossover preliminary study, *Circ. Heart Fail.* 3 (2010) 73–81.
- [21] L.G. Sanchez-Lozada, E. Tapia, V. Soto, C. Avila-Casado, M. Franco, J.L. Wessale, L. Zhao, R.J. Johnson, Effect of febuxostat on the progression of renal disease in 5/6 nephrectomy rats with and without hyperuricemia, *Nephron Physiol.* 108 (2008) 69–78.
- [22] S. Aslam, T. Santha, A. Leone, C. Wilcox, Effects of amlodipine and valsartan on oxidative stress and plasma methylarginines in end-stage renal disease patients on hemodialysis, *Kidney Int.* 70 (2006) 2109–2115.

